

Inversion of airborne electromagnetic survey data for sea-ice keel shape

Guimin Liu*, Austin Kovacs‡, and Alex Becker§

ABSTRACT

It is possible to interpret conventional airborne electromagnetic (EM) data acquired over ice-covered Arctic seas to obtain values of the sea ice thickness and, where needed, the actual sea ice keel geometry. To do so, we require high-frequency (inductive limit) data that allows us to assume that the ice is virtually transparent to the EM fields while the sea water forms a perfect conductor. Practically, a 100 kHz operating frequency is needed, but data acquired at a lower frequency can be scaled to obtain the required inductive limit anomaly. The data inversion is done by linking Occam's inversion method to a rapid numerical, two-dimensional, forward solution for the ice keel problem. A most useful feature of the adopted inversion scheme is the minimization of the roughness or

the mean square slope of the keel boundary. In some cases, where the keel might be bounded by steeply dipping walls, this constraint may result in a less accurate solution than might be obtained with a conventional technique. In most cases the advantage in stability that it provides outweighs the possible loss of accuracy that it may occasion. Tests on synthetic data show a possible worst case ice thickness error of about 15 percent. The results of inversion tests for two sets of survey data acquired near Prudhoe Bay, Alaska, also indicate an accuracy of this order of magnitude. While some portion of the inversion error must be ascribed to the roughness constraint and is therefore inherent to the inversion technique used, the remainder must be ascribed to the instrumentation and is probably remediable.

INTRODUCTION

Sea ice covers large areas of the Arctic and Antarctic seas. The thickness and distribution of this veneer as well as its physical and mechanical properties are of considerable importance. "Suffice it to say that ice thickness and its distribution influence components of the surface heat and momentum balance, the salt balance of the upper ocean, light penetration and biological productivity, and trafficability on top of, through, and beneath the ice cover," (Rothrock, 1981). On a more local scale, knowledge of the sea ice thickness and its topography along the sea-ice/seawater interface is important for the safe and efficient operation of ice breaking vessels and for the implantation of offshore drilling platforms.

It now appears, as shown by Kovacs et al. (1987) and Kovacs and Valleau (1987), that reliable information regarding the average sea-ice thickness may be routinely obtained with a conventional, helicopter-borne, electromagnetic pros-

pecting system. Going one step further, Liu and Becker (1990) showed that the observed data is affected by the presence of sea-ice keels and in particular how one may rapidly compute the electromagnetic anomaly produced by any given sea-ice keel.

In this paper, we will demonstrate the inverse process, namely the extraction of the sea-ice keel geometry from airborne electromagnetic (AEM) data. To do so we combine the rapid solution of the forward problem presented by Liu and Becker (1990) with Occam's inversion method proposed by Constable et al. (1987). This method finds the smoothest solution that is consistent with the observed data to a specified tolerance in the sense that the slopes of the recovered keel surface are minimized.

THEORY

Our purpose here is to reconstruct the distance from the AEM sensor to the ice-water interface $h(x)$ from the air-

Manuscript received by the Editor October 1, 1990; revised manuscript received May 28, 1991.

*Formerly Engineering Geoscience, University of California at Berkeley; presently BHP Research - ML, 245 Wellington Road, Mulgrave, VIC 3170, Australia.

‡United States Army, Cold Regions Research & Engineering Lab., Hanover, NH 03755-1290.

§Dept. of Material Science & Mineral Engineering, University of California at Berkeley, Berkeley, CA 94720.

© 1991 Society of Exploration Geophysicists. All rights reserved.

borne electromagnetic data $d(x)$, while the upper surface of the ice is mapped by a laser device. The difference in elevation between the bottom and the top surface of the ice is the required ice thickness. To do this we consider a two-dimensional (2-D) case where the keel has an infinite strike extent and the AEM profile is perpendicular to the keel strike. Furthermore, we assume that the survey data was either acquired at or scaled (Liu, 1989) to the inductive limit. This condition is usually reached at an operating frequency in excess of 100 kHz. We also assume that the interface between the insulating ice and the "perfectly" conductive water is sharp and distinct while the distance from this interface to the AEM sensor varies smoothly along the data profile. Under this assumption, any effects from the induced and channeled currents in sea ice are neglected.

In this case, one can, in principle, express the AEM data variation along the survey line as a function of the sensor-water distance along that line. More concisely, we can write

$$d(x) = F[h(x)] \quad (1)$$

where $F[\]$ is the functional relationship between $h(x)$ and $d(x)$. The problem at hand calls for the transformation of data acquired as a function of distance along a line into a set of relative elevations along the same line. The required result can be obtained by using Occam's inversion method introduced by Constable et al. (1987).

Occam's inversion is based on the search for a model of a given quantity [in our case, $h(x)$] that fits the observed data yet shows minimal local variation or first derivative values. This method applies particularly well to our work because electromagnetic wave propagation in sea water is a diffusion process, so that the resolution of sharp edges on the ice-water interface cannot be expected from the data. Furthermore, any information on sharp edges is contained in the high wavenumber range of the data where the signal-to-noise ratio is lowest. Because inversion implies downward continuation (Parker, 1977), any attempt to reconstruct the fine structure of the interface will amplify the noise and result in an unstable solution. Hence, a stable solution is necessarily smooth.

To find the smoothest solution, we will minimize the roughness of the ice-water interface. Thus we define the roughness of the interface to be

$$R = \int_{p_1}^{p_2} \left| \frac{dh(x)}{dx} \right|^2 dx.$$

The lateral keel extent outside of which the interface is assumed to be flat is given by the interval (p_1, p_2) . In the discrete sense,

$$R = \sum_{i=2}^N (h_i - h_{i-1})^2 = \|\underline{\partial}\mathbf{h}\|^2 \quad (2)$$

where $h_i = h(x_i)$, $\|\cdot\|$ denotes the ℓ_2 norm or root mean squared value, and

$$\underline{\partial} = \begin{bmatrix} 0 & 0 & 0 & \dots & 0 \\ -1 & 1 & 0 & \dots & 0 \\ 0 & -1 & 1 & \dots & 0 \\ \dots & \dots & \dots & \dots & \dots \\ 0 & 0 & \dots & -1 & 1 \end{bmatrix}$$

$$\mathbf{h} = (h_1, h_2, \dots, h_N)^T.$$

Note that $p_1 = x_1$, $p_2 = x_N$ and that the points x_1, x_2, \dots, x_N are usually equally spaced. Physically, the rougher the interface is, the larger the magnitude of its derivatives.

Suppose that there are M data points recorded over an ice keel, $d_j = d(x = X_j)$, $j = 1, 2, \dots, M$. Note that the values of X_j are usually different from those of x_j . The corresponding computed predictions from the discrete model \mathbf{h} are $F_j(\mathbf{h})$. The quality of fit of the predictions to the actual data can be evaluated using the least-squares criterion

$$E = \sum_{j=1}^M [d_j - F_j(\mathbf{h})]^2 = \|\mathbf{d} - \mathbf{F}(\mathbf{h})\|^2, \quad (3)$$

where

$$\mathbf{d} = (d_1, d_2, \dots, d_M)^T$$

$$\mathbf{F}(\mathbf{h}) = (F_1(\mathbf{h}), F_2(\mathbf{h}), \dots, F_M(\mathbf{h}))^T.$$

The ice-water interface \mathbf{h} can only vary within some physical bounds. If we assume that the $z = 0$ plane is chosen such that it coincides with the flat part of that interface then a reasonable lower bound is:

$$h_i \geq 0, \quad i = 1, 2, \dots, N \quad (4)$$

since the ice keel protrudes downward. An upper bound T_i can also be set for each individual case so that

$$h_i \leq T_i, \quad i = 1, 2, \dots, N. \quad (5)$$

In the Arctic, small ice keels may protrude several meters into the water, whereas large keels can protrude tens of meters. The values of T_i should be estimated for each specific ice keel encountered. Note that $h_1 = h_N = 0$ must be included in the constraints for the solution to be smooth at the two end points. This condition can be met by simply letting $T_1 = T_N = 0$.

Now, the mathematical problem to be solved can be stated as follows: find a solution \mathbf{h} that minimizes the roughness R and brings the misfit E within an acceptable tolerance, while the bound constraints of equations (4) and (5) are satisfied. Without the bound constraints, this problem is exactly identical to the one solved by Constable et al. (1987).

The condition for the data misfit is

$$\|\mathbf{d} - \mathbf{F}(\mathbf{h})\|^2 \leq E_* \quad (6)$$

where E_* is the tolerance. If we treat this inequality as an equality and apply the method of Lagrange multipliers, the above problem can be reduced to the minimization of

$$U = \|\underline{\partial}\mathbf{h}\|^2 + \mu^{-1}(\|\mathbf{d} - \mathbf{F}(\mathbf{h})\|^2 - E_*) \quad (7)$$

with constraints of equations (4) and (5). Here μ^{-1} is the Lagrange multiplier. As interpreted by Constable et al., μ is

a smoothing parameter. The larger μ is, the less the solution is affected by the misfit. On the contrary, if μ is small, the data misfit is dominant while the influence from the roughness R is relatively weak.

The original problem can now be solved with the following procedures: Solve the above minimization problem for a preselected series of μ values to obtain a set of solutions for the ice-water interface, $h(x)$. Among these solutions, choose the one that satisfies the tolerance condition in equation (6). If more than one solution satisfies equation (6), choose the one with the largest μ value, for this corresponds to the desired smoothest solution.

Such solutions cannot however be easily obtained by the direct minimization of the objective function U [equation (7)] since the minimization is nonlinear. It is first necessary to transform the nonlinear problem into a problem of quadratic programming, for which existing mathematical tools can be used.

Let us linearize the functional $\mathbf{F}(\mathbf{h})$ about an initial model \mathbf{h}^0

$$\mathbf{F}(\mathbf{h}) = \mathbf{F}(\mathbf{h}^0) + \mathbf{J}\Delta \quad (8)$$

Here Δ is the correction to be applied to \mathbf{h}^0 ; $\mathbf{h} = \mathbf{h}^0 + \Delta$; and \mathbf{J} is the Jacobian matrix of the partial derivatives. Substituting equation (8) into equation (7) and dropping the constant term $\mu^{-1} E_*$, we obtain

$$U = \|\tilde{\mathbf{d}}\|^2 + \mu^{-1} \|\tilde{\mathbf{d}} - \mathbf{J}\mathbf{h}\|^2$$

where $\tilde{\mathbf{d}} = \mathbf{d} - \mathbf{F}(\mathbf{h}^0) + \mathbf{J}\mathbf{h}^0$ is the modified data. Rearrangement of the above equation gives

$$V = \frac{1}{2} \mu U - \tilde{\mathbf{d}}^T \tilde{\mathbf{d}} = \frac{1}{2} \mathbf{h}^T \mathbf{H} \mathbf{h} - \mathbf{C}^T \mathbf{h}. \quad (9)$$

Here V is the new objective function and

$$\mathbf{H} = \mu \tilde{\mathbf{d}}^T \tilde{\mathbf{d}} + \mathbf{J}^T \mathbf{J}$$

$$\mathbf{C} = \mathbf{J}^T \tilde{\mathbf{d}}.$$

Note that \mathbf{H} is a symmetric positive-definite matrix. The minimization of the new objective function V is equivalent to the minimization of U for a fixed value of μ .

Now that the new objective function is in quadratic form, the problem of optimization with bound constraints of equations (4) and (5) can be solved using quadratic programming (Gill et al., 1981). There are subroutines available in existing mathematical software libraries that can be used for this purpose. These are E04AF in the NAG Fortran Library and VE04A in the Harwell Fortran Library. We selected VE04A because of its simplicity.

The smoothest solution can now actually be obtained in the following way. Starting from an initial model \mathbf{h}^0 , solve the minimization problem for different μ values. From these solutions choose the one that minimizes the actual misfit E instead of V . [Minimizing V may result in divergence of the solution (Constable et al., 1987)]. Use this solution for the next initial model and repeat the entire procedure until the solution for the ice-water interface topography that brings the misfit below a specified tolerance is found.

The initial model \mathbf{h}^0 can be chosen arbitrarily since it does not appear to affect the convergence of the inversion to the smoothest solution. This is one of the beauties of the smooth inversion scheme which sets out to seek a unique solution. In our problem we set the initial model to be a flat ice cake, i.e., $\mathbf{h}^0 = (0, 0, \dots, 0)^T$.

THE AEM SYSTEM

The AEM system works on the principles of electromagnetic induction. A transmitter coil is excited by a sinusoidal electric current and produces an alternating magnetic field in space so that currents are then induced in any nearby conductors (e.g., sea water). These induced currents in turn produce a secondary magnetic field which is sensed by the receiver coil and recorded digitally on a magnetic tape. A part of the transmitting current is fed into the recording electronics to buck out the primary magnetic field at the receiver. Using this technique, the secondary field can be measured with high precision so that its in-phase and quadrature components are recorded in parts per million (ppm) of the primary magnetic field with a precision of one ppm. These data are used to determine the height of the system above the sea water surface. At the same time the system altitude above the snow surface is measured by a laser altimeter. Thus the snow plus ice thickness is obtained from a difference in these two quantities.

A conventional, helicopter-borne, AEM system is a multicoil multifrequency instrument that is principally used for mineral exploration (Fraser, 1979). It normally consists of a "bird," which is a plastic tube that contains a number of coil pairs and is suspended on a cable below the helicopter and the system electronics housed in the aircraft. Each coil pair consists of a transmitter and a receiver separated by a fixed distance and operating at a distinct frequency. The system is usually based on three or more coil pairs some of which are arranged in the horizontal coplanar mode while others are positioned in the vertical coaxial mode. In operation, the bird is towed about 30 m below the helicopter which flies at an altitude of about 60 m above the sea ice surface.

In this paper we consider both synthetic results and field data. The synthetic results are computed at the inductive limit for a coplanar system with a coil separation of 6.5 m. The field data was obtained in 1987 by Kovacs and Holliday (1990) using a short 3.5 m bird which was 35 cm in diameter. It contained two coplanar coil sets that operated at 811 Hz and 50 kHz and one coaxial coil set that operated at 4.5 kHz. In all cases, the transmitter-receiver separation was held at 3 m. This system was fabricated by Geotech Limited of Toronto, Canada.

FIELD SURVEY ACTIVITIES

Prior to the airborne survey, extensive information was collected at a number of sea ice sites near Prudhoe Bay, Alaska over which AEM flights were subsequently made. This information included snow depth, temperature, and conductivity. Two of these sites and the related AEM sounding data are discussed in this paper. One site was on first-year sea ice and the second was on a multiyear sea-ice floe. Both sites included a pressure ridge and the associated

sea ice keel. A detailed description of the test sites is given by Kovacs and Holladay (1990).

At each site a 50-m-wide track line was laid out by standard survey methods. The track length on the multiyear sea-ice floe was 200 m. At the first-year pressure ridge site, the track length was 230 m. The track was divided into 11 longitudinal lines spaced 5 m apart. At 5-m intervals along each line, the snow and ice thickness as well as the freeboard were determined by drill-hole measurement. These drill-hole data were then used to construct an average cross-section of the snow cover, the ice freeboard and draft along each grid length.

To make a proper comparison between the drill hole data and the ice thickness estimates obtained from the electromagnetic measurements, one must allow for the AEM system footprint. As shown by Kovacs et al. (1987) and Liu and Becker (1990), this quantity can be represented by a circle whose diameter is about 1.5 times the height of a coaxial system and a circle about three times the height of the coplanar system. In the present case, the coplanar system was flown at about 25 m above the ice-water interface so that the system footprint was taken to be about 75 m. For the purpose of comparison between airborne and ground data, we took the arithmetic average of the drill-hole results for the seven drill-hole lines adjacent and parallel to the helicopter track.

DATA PROCESSING

Once the acquired data is properly calibrated and corrected for any instrumental drift, it must be adjusted or scaled to estimate the inductive limit response of the ice-water interface topography from the measured high-frequency response. A good way to do this for data acquired at 50 kHz or higher frequencies is simply to augment the observed in-phase response by the corresponding observed values of the quadrature response (Becker et al., 1983). A more complicated scaling procedure (Liu, 1989) must be used to adjust data recorded at lower frequencies. Nonetheless, good values of the inductive limit response can be obtained from measurements made at frequencies as low as 4.5 kHz.

The adjusted data may now be interpreted even though it was acquired at a variable altitude. On the other hand for purpose of inspection, or other reasons, one may first wish to remove the altitude effects so that the corrected data principally represents the effect of the snow plus sea ice thickness variations. This can be readily done using the complex image source concept put forward by Thomson and Weaver (1975). The results of this procedure, which is described by Liu and Becker (1989), are shown in Figure 1 that sequentially presents the altimeter data, the observed 50 kHz coplanar system AEM data, and the altitude corrected data. This data was acquired on line F14L3 over the first-year sea ice and pressure ridge site and when corrected for altitude variations clearly indicates a prominent keel at fiducial 3075. Its presence is not readily observable in the original data. Additionally, we note that the difference in background levels to the left and to the right of the keel anomaly is read and correctly corresponds to an approxi-

mate 80 cm increase in snow plus ice thickness to the right of the indicated keel.

DATA INTERPRETATION

Synthetic results

To test the proposed inversion technique, we first consider a synthetic data set generated for a triangular keel using a procedure outlined by Liu and Becker (1990). The results are computed at the inductive limit for a coplanar vertical dipole system that is about twice as long as the system used in the field and has a coil separation of 6.5 m. The system height over the ice surface is taken as 25 m. The model consists of a symmetric triangular keel with a 30 m base and a 5 m drawdown (Figure 2). It is covered by a 5 m thickness of uniform ice so that the maximum ice thickness for this model is 10 m. The synthetic data are generated at intervals of 3.5 m that corresponds to a rate of 10 points/s at a helicopter speed of 68 knots.

Once the synthetic data is generated, the first step in the inversion procedure is the selection of the end points p_1 , p_2 that define the initial guess of the keel width. For the coplanar system, these should be taken to correspond to the points at which the related AEM anomaly falls to one half of its maximum amplitude. In the present case, these fall at about 45 and 105 m along the profile shown in Figure 2. Next, the sampling interval along the ice-water interface is taken as 3 m allowing the keel to be defined by 21 depth values which are all initially assumed to equal 5 m. After three iterations of the inversion process the results converge to the keel shape shown in the lower part of Figure 2 which also shows the original triangular model. The upper portion of this illustration compares the synthetic data input (solid line) with the theoretical response for the interpreted model.

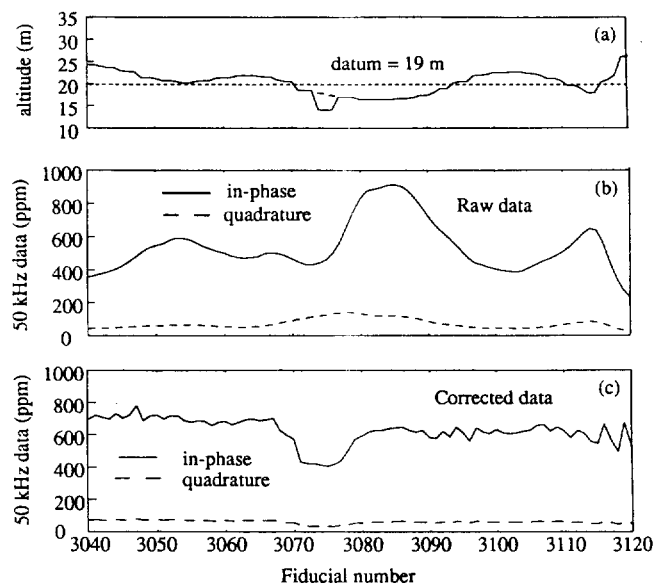


FIG. 1. Coplanar, 50 kHz AEM data along line F14L3. (a) Laser altimeter record with an indication of the 19 m data reduction level. (b) Observed in-phase and quadrature data. (c) Observed data corrected to the 19 m datum level.

A 2 ppm rms fit criterion was used to test convergence. The inversion result is, as expected, much smoother than the input model. Because the inversion procedure smooths out the apex of the keel, the interpreted ice thickness is 1.5 m shallower than the triangular keel model used to compute the synthetic data. Obviously if the slope of the keel were steeper than the approximate 18-degree slope of this idealized keel, the interpreted thickness would be shallower still. It should also be noted, that in this case, the synthetic data were noise free. Liu (1989) however, considered the same example where the synthetic data were degraded by the addition of about 13 ppm rms (5 percent) noise. Noise, at that level, did not have a significant influence on the recovered model.

Field data

Now we apply the inversion method to the 50 kHz AEM data acquired along line F14L3 over a first-year ridge. The anomaly centered on fiducial 3075 was assumed to be related to a 2-D keel bounded by two uniform ice sheets of differing thickness (1.5 m on the left; 2.3 m on the right). The data for the inversion was taken at 27 points defined by fiducial marks 3065 to 3091 inclusive. A 4-m sampling interval was used to discretize the ice-water interface in the keel region. In this case, (because of the asymmetric anomaly) it was

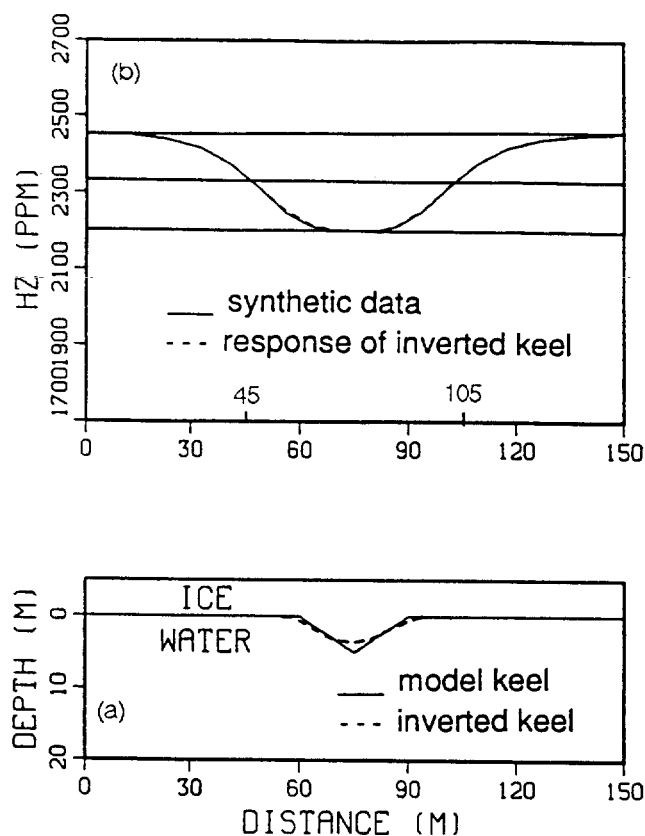


FIG. 2. (a) Triangular model keel and its recovered smoothed version beneath a 5 m thick uniform ice layer. (b) Synthetic coplanar data for model keel (solid line) and theoretical anomaly for the recovered keel (dashed line).

found useful to allow a larger initial value for the keel width than indicated by the anomaly shape. It was therefore assumed that the keel base lies between fiducials 3068 and 3083 that correspond to the 30 and 118 m points along the test profile.

The results of the inversion along with a comparison of model response and field data are shown in Figure 3. Although the fit between the field data and the model response is quite good, the interpreted keel is shallower than indicated by the drilling results. In particular, we find that the inversion yields an overall snow and ice thickness of only 13.5 m which is some 4 m less than the snow and ice thickness indicated by drilling. Furthermore, the interpreted keel is noticeably offset from its true position. This rather inaccurate result may be related to the higher electrical conductivity and to the steeper keel slope of first-year ice keels (Kovacs and Holladay, 1990). The interpreted ice thickness however is still more indicative of the true ice thickness than the value of only about 10 m that is obtained from a simpler, layered model analysis of the same data (Kovacs and Holladay, 1990).

A much more encouraging interpreted result is obtained using data acquired over the multiyear Floe 3. Here we take 50 kHz data between fiducials 5401 and 5414 of line F13L8 (Figure 4) and apply the inversion technique to define the ice keel that is centered near fiducial mark 5410 and is assumed to lie between 78 and 186 m along the test profile. Once again the ice-water interface along this interval was digitized at 4 m

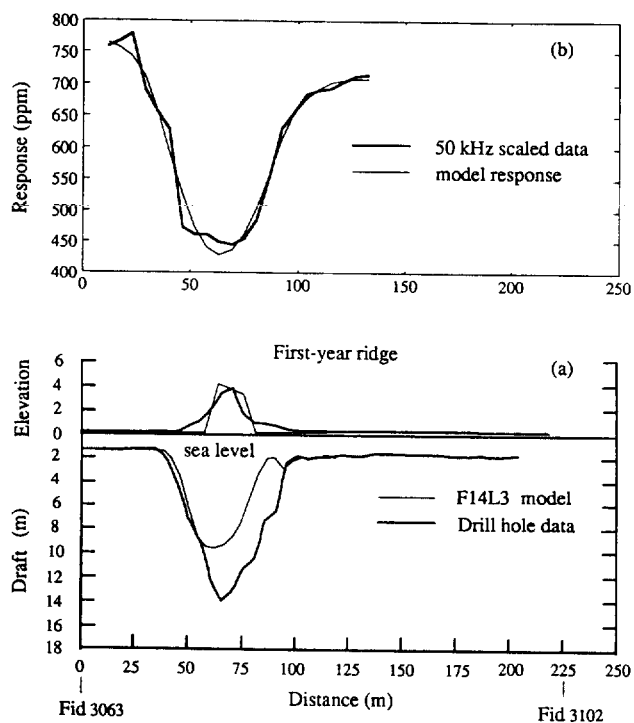


FIG. 3. (a) Comparison of drill hole data for first-year ice keel and the keel model recovered from survey data along line F14L3. The ridge on the top of the keel model was recovered from the altimeter record. (b) Comparison of observed AEM data and the theoretical AEM anomaly for recovered keel model.

intervals. A uniform thickness of 3.6 m was assigned to the ice in which the keel is embedded. The results of the inversion and the comparison of the observed data with the numerical model results are shown in Figure 4. Here we find a fairly good agreement between the interpreted ice keel shape and the drilling results. As expected, because of the smoothness requirements of the inversion process, the interpreted keel shape is smoother than indicated by drilling. Nonetheless the predicted snow-ice thickness of about 7 m compares favorably with the 8 m maximum thickness obtained from the drill-hole data.

CONCLUSIONS

On the basis of the results shown above we conclude that one can interpret airborne electromagnetic data in terms of sea-ice keel geometry with a reasonable degree of success. Although the accuracy with which the maximal snow plus ice thickness was determined in the two available test cases (23 percent and 12 percent respectively) was much poorer than the best accuracy value of 5 percent that can be anticipated in areas of uniform ice thickness (Kovacs and Holladay, 1990), it is much better than the accuracy that would have been obtained had we tried to use any simpler method of analysis.

There are a number of possible reasons for the discrepancy between the inversion results and the drilling data.

These fall into two categories. The first one encompasses inadequacies in the model used for the inversion. Here because the lowermost portion of a first-year keel is porous and therefore of higher bulk salinity, its electrical conductivity is probably quite different from the assumed value of zero. Some of the problem may be related to the smoothness requirements implicit to the inversion technique, to keel slope steepness and to the fact that first-year pressure keels do not have a well defined ice-water interface. Another source of error in this area, which probably does not apply in the two cases examined, is the finite strike length of any keel. As shown by Liu and Becker (1990) the assumption of a truly two-dimensional structure is not valid for keels whose strike length is shorter than three times the system height above the ice-water interface. The second group of error sources relates to the instrumentation itself. Among the problems to be considered here we have the lack of correction for the pitch and roll of the bird, excessive system noise and drift and distortion of the recorded anomaly shape by excessive signal averaging along the flight path. In addition, as pointed out by Kovacs and Holladay (1990), there is the inability of the laser profiler to assess the average system elevation above the variable surface topography enclosed within the system footprint.

ACKNOWLEDGMENT

Funding for this study was provided by the U.S. Department of Navy, Naval Oceanographic and Atmospheric Research Laboratory, under the contracts N0014-87-K-6005 and N6845286-MP60003.

REFERENCES

- Becker, A., Morrison, H. F., and Smits, K., 1983, Analysis of airborne electromagnetic systems for mapping thickness of sea ice: Nav. Ocean Res. and Develop. Act., Tech. note 261.
- Constable, S. C., Parker, R. L., and Constable, C. G., 1987, Occam's inversion: A practical algorithm for generating smooth models from electromagnetic sounding data: *Geophysics*, **52**, 289-300.
- Fraser, D. C., 1979, The multicoil II airborne electromagnetic system: *Geophysics*, **44**, 1367-1394.
- Gill, P. E., Murray, W., and Wright, M. H., 1981, Practical optimization: Academic Press Inc.
- Kovacs, A., and Holladay, J. S., 1990, Sea-ice thickness measurement using a small airborne electromagnetic sounding system: *Geophysics*, **55**, 1327-1337.
- Kovacs, A., and Valleau, N., 1987, Airborne measurement of sea-ice thickness and sub-ice bathymetry: The 9th Conference in Port and Ocean Engineering Under Arctic Conditions, University of Alaska, Fairbanks, Alaska.
- Kovacs, A., Valleau, N., and Holladay, J. S., 1987, Airborne electromagnetic sounding of sea-ice thickness and sub-ice bathymetry: *J. Cold Reg. Sci. and Tech.*, **14**, 289-311.
- Liu, G., 1989, Airborne electromagnetic sensing of sea ice thickness: Ph.D. thesis, Univ. of California at Berkeley.
- Liu, G., and Becker, A., 1990, Two-dimensional mapping of sea-ice keels with airborne electromagnetics: *Geophysics*, **55**, 239-248.
- Liu, G., and Becker, A., 1989, Interpretation of AEM data in terms of ice keel geometry: Univ. of California at Berkeley, Eng. Geosci. Rep.
- Parker, R. L., 1977, Understanding inverse theory: *Ann. Rev. Earth Sci.*, **5**, 35-64.
- Rothrock, D. A., 1981, Ice thickness distribution—measurement and theory, in: Untersteiner, N., Ed., *Geophysics of sea-ice*: Plenum Press, 551-575.
- Thomson, D. J., and Weaver, J. T., 1975, The complex image approximation for induction in a multilayered earth: *J. Geophys. Res.*, **80**, 123-129.

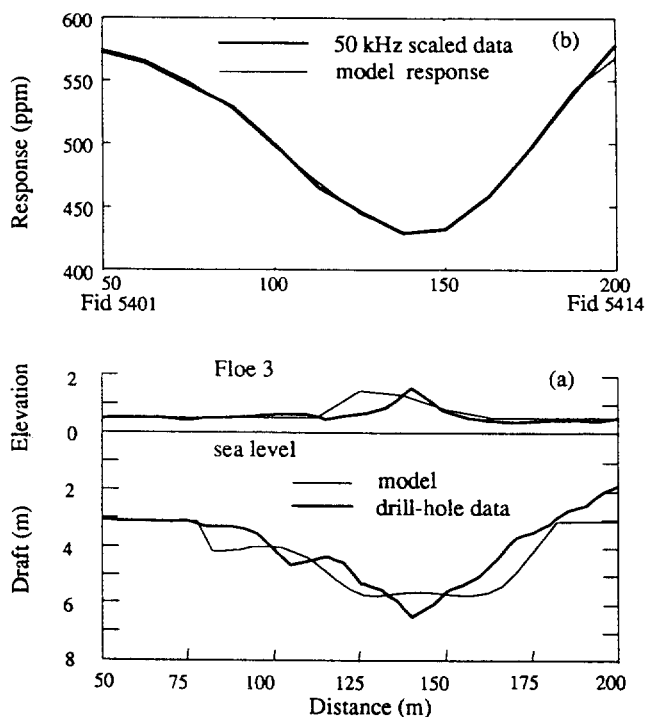


FIG. 4. (a) Comparison of drill hole data for multiyear ice keel observed beneath Floe 3 and its model as recovered from AEM data. The ridge on the top of the keel model was recovered from the altimeter record. (b) Correspondence of observed and scaled 50 kHz AEM data and the theoretical anomaly computed for the recovered model.